BAREKENG: Journal of Mathematics and Its Applications
September 2026 Volume 20 Issue 3 Page 1967-1984
P-ISSN: 1978-7227 E-ISSN: 2615-3017
https://doi.org/10.30598/barekengvol20iss3pp1967-1984

A MATHEMATICAL MODEL OF DIPHTHERIA TRANSMISSION DYNAMICS WITH HETEROGENEOUS SUSCEPTIBILITY

Mohamad Tafrikan [1], Fatmawati [2*], Windarto [3], Chinwendu E. Mudubueze [4]

[1,2,3]*Department of Mathematics, Faculty of Science and Technology, Universitas Airlangga*
Jln. Dr. Ir. H. Soekarno, Mulyorejo, Surabaya, 60115, Indonesia

[1]*Department of Mathematics, Faculty of Science and Technology, Universitas Islam Negeri Walisongo*
Jln. Walisongo No 3-5 Semarang, Jawa Tengah, 50185, Indonesia

[4]*Department of Mathematics, Joseph Sarwuan Tarka University*
QJQ8+XXW, Makurdi, 970101, Nigeria

*Corresponding author's e-mail: *fatmawati@fst.unair.ac.id*

Article Info

Article History:

Received: 11th July 2025
Revised: 21th December 2025
Accepted: 16th March 2026
Available online: 8th April 2026

Keywords:

Diphtheria disease;
Mathematical model;
Stability analysis;
Parameter estimation;
Vaccination

ABSTRACT

Despite the availability of vaccines, diphtheria continues to pose a public health risk in Indonesia due to uneven vaccination coverage across regions. Previous models have not distinguished between highly susceptible (unvaccinated) and susceptible (vaccinated) populations, nor have they been calibrated with actual Indonesian epidemiological data. To address this gap, this study develops a five-compartment diphtheria transmission model: Highly susceptible (unvaccinated)-Susceptible (vaccinated)-Exposed-Infectious-Recovered (S_1 S_2 EIR), which incorporates two levels of susceptibility based on vaccination status, using empirical diphtheria case data in Indonesia from 2012 to 2023. The analysis begins by proving the positivity, boundedness, and uniqueness of solutions, followed by the calculation of the basic reproduction number using the Next-Generation Matrix method. The analysis shows that the disease-free equilibrium (DFE) is locally and globally asymptotically stable when $R_0<1$, while the endemic equilibrium (EE) is globally stable when $R_0>1$. Simulations indicate that the interaction parameter for the unvaccinated group η_1, strongly accelerates epidemic growth, leading to a higher and earlier infection peak, whereas increased vaccination coverage and recovery rates effectively suppress transmission. This model can be used because the Mean Absolute Percentage Error (MAPE) between the data and the model solution for diphtheria cases in Indonesia is 8.77%. These results highlight the importance of interventions focused on highly susceptible groups to prevent more severe outbreaks. Therefore, this study is significant in strengthening the theoretical understanding of diphtheria transmission, while also providing data-driven insights as recommendations for policymakers to implement effective and efficient outbreak control measures.

How to cite this article:

M. Tafrikan, Fatmawati, Windarto and Chinwendu E. M., "A MATHEMATICAL MODEL OF DIPHTHERIA TRANSMISSION DYNAMICS WITH HETEROGENEOUS SUSCEPTIBILITY", *BAREKENG: J. Math. & App.*, vol. 20, no. 3, pp. 1967-1984, Sep, 2026.

Journal homepage: *https://ojs3.unpatti.ac.id/index.php/barekeng/*
Journal e-mail: *barekeng.math@yahoo.com; barekeng.journal@mail.unpatti.ac.id*
Research Article · Open Access

1. INTRODUCTION

Diphtheria is a bacterial infection caused by Corynebacterium diphtheriae, which can be prevented through vaccination [1], [2]. Transmission occurs via respiratory droplets (e.g., sneezing or coughing), direct contact with infected skin, or contaminated objects [2]. Additionally, asymptomatic individuals may transmit the pathogen for up to four weeks post-exposure [3]. Clinical manifestations typically emerge within 2–5 days post-exposure, ranging from mild to severe presentations, including breathing difficulties, trouble swallowing, and persistent coughing. In severe cases, complications like heart inflammation, nerve damage, and kidney failure may arise [4]. Even the case fatality rate among unvaccinated individuals without treatment may reach 50%, but timely treatment reduces it to approximately 10% [5].

Vaccination has been demonstrated to be the most effective preventive intervention [6], with a three-dose booster series recommended during childhood and adolescence. Therefore, public health initiatives prioritizing parental education regarding routine immunization may contribute to reduced transmission rates. [7]. In Indonesia, a total of 7,886 diphtheria cases and 339 deaths were recorded between 2012 and 2023, with the highest incidence reported in 2018 (1,386 cases) and the highest mortality observed in 2022 (46 deaths). However, vaccination coverage remains uneven across regions, including Papua (29.6%) and Aceh (49.6%) [8]. Low vaccination rates in these areas indicate the presence of population groups with a substantially higher risk of infection compared to regions with better coverage. In addition to vaccination, natural immunity strengthened through good nutrition, healthy habits, and adequate sanitation also plays an important role in prevention, in line with the guidelines of the Indonesian Ministry of Health. To effectively address this persistent public health challenge, a deeper understanding of the disease's transmission dynamics is crucial. In this context, mathematical modeling provides a valuable framework for analyzing diphtheria spread and evaluating control strategies.

Mathematical modeling represents real-world conditions into mathematical equations [9]. As epidemiological models described by [10], it simulates disease transmission to identify transmission patterns and predict outbreaks, as well as assisting in the optimization of interventions. In addition, the transmission of infectious diseases can be mathematically modeled using the Susceptible-Infected-Recovered (SIR) framework, which was first introduced by Kermack and McKendrick [11]. The SIR model was later developed by Hethcote [12], who maintained the fundamental assumption of a closed population. Diphtheria transmission models also apply this approach by structuring disease dynamics within a mathematical framework.

Various compartmental models have been used to study diphtheria transmission, and they consistently show that vaccination and quarantine reduce transmission. For example, Susceptible-Infected-Recovered-Quarantined (SIQR) analyses indicate that a vaccination rate above 0.884 and a cure rate greater than 0.04 are required to suppress outbreaks [13], while vaccine impact studies, including historical data from the former Soviet Union in 1990 [14] and analyses of Thai data [15] - [18], report reductions in infections due to vaccination. Similarly, study [21], which examined a Susceptible-Infectious-Recovered-Deceased (SIRD) model incorporating vaccination, shows that high vaccination coverage significantly reduces diphtheria transmission. Furthermore, studies using the Susceptible-Exposed-Infectious-Quarantined-Recovered (SEIQR) model demonstrate that quarantining exposed individuals can suppress transmission through natural immunity [19] - [20]. However, the Susceptible–Exposed–Infectious–Recovered (SEIR) model used in [22] allows reinfection even when quarantine interventions are applied. The results of that model also show the presence of an endemic steady state in diphtheria transmission dynamics. A recent study by [23], which examined the effect of migration on the spread of diphtheria infection in Mandau District, shows that the resulting mathematical model is stable and simulations indicate that the spread of infection can be halted by 2030.

Based on the explanation above, no previous studies have distinguished two susceptibility classes based on vaccination status. In addition, most studies have not used actual Indonesian epidemiological data, making them unable to capture the variation in risk arising from uneven vaccination coverage across regions. To address these limitations, this study develops a five-compartment: Highly susceptible (unvaccinated)-Susceptible (vaccinated)-Exposed-Infectious-Recovered (S_1S_2EIR) model as a modification of the SEIR model by dividing the susceptible class into S_1 (highly susceptible (unvaccinated)) and S_2 (susceptible (vaccinated)), incorporating vaccination-dependent transmission parameters, and calibrating the model using empirical diphtheria case data from Indonesia from 2012 to 2023. This formulation represents a novel contribution by capturing population heterogeneity more realistically and providing a data-driven framework

for analyzing diphtheria transmission dynamics under Indonesia's epidemiological conditions. To evaluate the proposed model, the analysis first verifies solution feasibility, uniqueness, and positivity. The disease-free equilibrium is shown to be locally and globally asymptotically stable. Using Lyapunov functions, the global asymptotic stability of the endemic equilibrium is established. Parameters are estimated via least-squares regression, followed by numerical simulations to visualize transmission trends. Consequently, this study not only strengthens the theoretical understanding of diphtheria transmission but also offers evidence-based insights that can support policymakers in designing effective and efficient outbreak control strategies.

2. RESEARCH METHODS

The research method for analyzing the stability of a mathematical model for diphtheria transmission in Indonesia is given as follows

2.1 Mathematical Model of Diphtheria Disease Spread

This study develops a deterministic compartmental model to analyze the transmission dynamics of diphtheria in Indonesia. The total population is stratified into five distinct epidemiological compartments:

S_1 : Highly susceptible individuals (unvaccinated)
S_2 : Susceptible individuals (vaccinated)
E : Exposed individuals (infected but not yet infectious)
I : Infectious individuals
R : Recovered individuals with immunity

The model assumes a closed population with a constant recruitment (birth) rate μ and natural death rate δ. Individuals are vaccinated at birth with a proportion g, leading to $(1-g)$ representing the unvaccinated. The interaction between infectious individuals and susceptible populations leads to new exposures, with different interaction rates η_1 and η_2 for unvaccinated and vaccinated susceptibles, respectively. Exposed individuals progress to the infectious stage at rate β, while infectious individuals either recover at rate γ or die from disease at rate θ.

2.2 Model Assumptions

The model assumptions in determining the spread of diphtheria in this study are:

1. The model assumes a closed population with a constant recruitment (birth) rate μ and natural death rate δ.
2. Natural mortality rate is assumed to be the same for each subpopulation.
3. Mortality rate is divided into two categories: natural mortality and mortality due to diphtheria.
4. The rate of increase of the subpopulation into the diphtheria disease dynamics system comes from individuals of all ages.
5. The model explains the dynamics of diphtheria spread by distinguishing susceptible groups into two categories: highly susceptible (individuals who have not been vaccinated) and susceptible (individuals who have been vaccinated).
6. The vaccinated susceptible subpopulation and the highly susceptible (unvaccinated) subpopulation can become infected with diphtheria due to interaction with the infected subpopulation, thus entering the Exposed (E) subpopulation with different interaction rates.
7. The recovered subpopulation with immunity is assumed to be unable to be reinfected.

2.3 Proposed Mathematical Model

In this model of diphtheria transmission, at the initial stage, the population grows in accordance with the birth rate (μ). The parameter g represents the proportion of the population that has received vaccination, implying that $(1-g)$ corresponds to the unvaccinated segment. The rates at which highly susceptible and susceptible individuals come into contact with infected individuals are denoted by η_1 and η_2, so that Exposed individuals (E) can increase with the interaction between susceptible and infection individual by $(\eta_1 S_1 + \eta_2 S_2)I$.

Exposed individuals (E) can change their status to infected (I) by βE, where β is the infection rate. Infected individuals (I) can increase by βE and can decrease due to death caused by diphtheria by θI, where θ is the death rate due to diphtheria. On the other hand, individual (I) can also decrease due to recovery from the disease by γI, where γ is the rate of individuals recovering. The number of recovered individuals R can increase by γI. Each individual can decrease due to natural death by a rate of δ. The detailed definition of each parameter notation is explained in Table 1. Furthermore, the compartment diagram of the diphtheria spread model in this study is presented in Fig. 1.

Table 1. Definition of Model Parameters

Notation	Description
g	Proportion of vaccinated individuals in the population
μ	Natural increase rate
δ	Natural death rate
η_1	Interaction rate between highly susceptible subpopulations and infected subpopulations
η_2	Interaction rate between susceptible subpopulations and infected subpopulations
β	Infection/transmission rate
γ	Recovery rate
θ	Death rate due to diphtheria

Based on the description above, a non-linear differential equation system is formed for the diphtheria disease spread model as follows:

$$\begin{aligned}
\frac{dS_1(t)}{dt} &= (1-g)\mu - (\delta + \eta_1 I)S_1, \\
\frac{dS_2(t)}{dt} &= g\mu - (\delta + \eta_2 I)S_2, \\
\frac{dE(t)}{dt} &= (\eta_1 S_1 + \eta_2 S_2)I - (\beta + \delta)E, \\
\frac{dI(t)}{dt} &= \beta E - (\gamma + \delta + \theta)I, \\
\frac{dR(t)}{dt} &= \gamma I - \delta R.
\end{aligned} \tag{1}$$

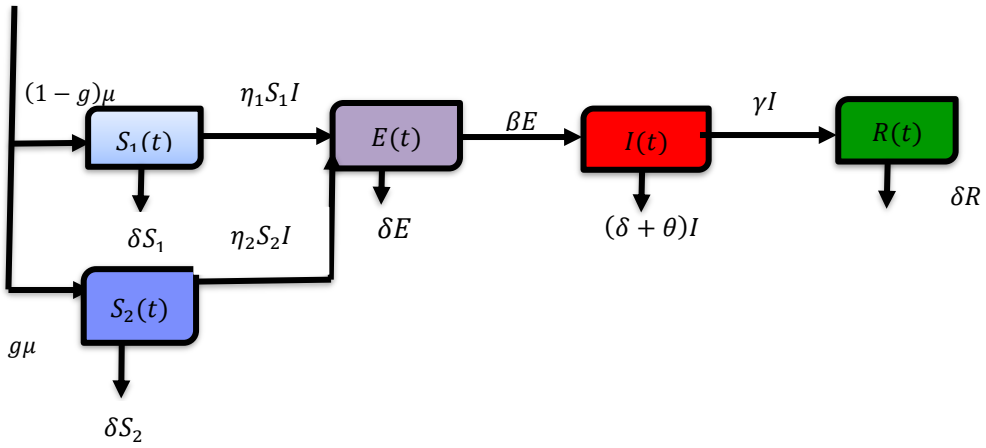

Figure 1. Compartment Diagram of Diphtheria Epidemic Model

with

⟶ : Reducing the population of origin and increasing the population of goals

2.4 Equilibrium Point and Stability Analysis

Two equilibrium states are analyzed:

1. Disease-Free Equilibrium (DFE): All individuals are susceptible, and there is no infection.

2. Endemic Equilibrium (EE): Infection persists in the population, and all compartments reach a steady state.

The basic reproduction number $\mathcal{R}_0$ is derived using the Next Generation Matrix method. It quantifies the average number of secondary cases generated by one infected individual in a completely susceptible population. The system exhibits:

1. Local stability of the DFE when $\mathcal{R}_0 < 1$, confirmed using Jacobian eigenvalues and the Routh-Hurwitz criteria.
2. Global stability of the DFE using Lyapunov functions and LaSalle's Invariance Principle
3. Global stability of the endemic equilibrium when $\mathcal{R}_0 > 1$, also proven using a carefully constructed Lyapunov function.

2.5 Data Sources and Parameter Estimation

Empirical data on diphtheria cases in Indonesia (2012–2023) were used for parameter fitting. Demographic parameters (μ, g, δ) were derived from national statistics including birth rates, life expectancy, and vaccination coverage among children aged 0–9. The remaining parameters $(\eta_1, \eta_2, \beta, \gamma, \theta)$ were estimated using the least squares method. This involved minimizing the squared error between model predictions and reported cumulative diphtheria cases. The initial conditions and parameter values were adjusted iteratively to obtain the best fit.

2.6 Numerical Simulations and Sensitivity Analysis

Numerical simulations were conducted to:

1. Compare model predictions with actual data.
2. Analyze the effects of varying parameters $(\eta_1, \eta_2, \mu, \gamma, \theta)$ on the dynamics of the infected population.
3. Evaluate sensitivity of each parameter to the basic reproduction number $\mathcal{R}_0$.

This section outlines the development process of a mathematical model aimed at understanding the transmission patterns of diphtheria. The analysis proceeds by identifying the disease-free equilibrium and the conditions under which the disease becomes endemic. It also involves calculating the basic reproduction number $\mathcal{R}_0$, analyzing local stability in both disease-free and endemic scenarios, performing numerical simulations, and interpreting the resulting graphical outputs.

3. RESULTS AND DISCUSSION

This section presents the main findings of this study. We begin with a discussion of positivity, boundedness, and uniqueness of solutions, parameter estimation, equilibrium point, stability of disease-free equilibrium point, endemic equilibrium, endemic global stability, and numerical simulation. The following is a detailed explanation of each subtopic:

3.1 Positivity, Boundedness and Uniqueness of Solutions

Theorem 1. *Assume that* $S_1(0), S_2(0), E(0), I(0)$,*and* $R(0)$ *are the initial condition system of Eq. (1). If* $S_1(0), S_2(0), E(0), I(0)$, *and* $R(0) \geq 0$, *then the solution remains non-negative for all* $t \geq 0$.

Proof. Carry out the first equation of the system Eq. (1) becomes:

$$\frac{dS_1(t)}{dt} - \big(-(\delta + \eta_1 I)\big)S_1 = (1-g)\mu. \tag{2}$$

We obtain,

$$\frac{dS_1(t)}{dt} \geq -(\delta + \eta_1 I)S_1,$$

$$\Leftrightarrow S_1(t) \geq S_1(0)e^{\int -(\delta+\eta_1 I)dt}. \tag{3}$$

Hence, $S_1(0)$ and $e^{\int -(\delta+\eta_1 I)dt}$ are non-negative for $t \geq 0$, then $S_1(t) \geq 0$. In the same way, it can be shown that $S_2(0), E(0), I(0)$, and $R(0) \geq 0$. ■

Next, it will be proven that Ω is bounded, add up all the equations in system of Eq. (1), we get

$$\frac{dN}{dt} - (\mu - N\delta) = -\theta I, \tag{4}$$

which implies

$$N \leq \frac{\mu}{\delta} + \frac{(\delta N_0 - \mu)e^{-\delta t}}{\delta}, \tag{5}$$

for $t \to \infty$, so $N(t) = \frac{\mu}{\delta}$. We can conclude that the solution set of Eq. (1) Ω is bounded. To demonstrate the uniqueness of the solution to Eq. (1), we prove an inequality involving $\| F(T) - F(\bar{T})\| \leq L\|T - \bar{T}\|$ with $\bar{T} = (\bar{S_1}, \bar{S_2}, \bar{E}, \bar{I}, \bar{R})$, $F(T) = \big(F_1(T), \dots, F_5(T)\big)$, and L are respectively the solution set of Eq. (1) when the equilibrium condition is reached, the mapping function or interaction between sub-populations, and a positive constant [24], where

$$\begin{aligned} F_1(T) &= (1-g)\mu - (\delta + \eta_1 I)S_1, \\ F_2(T) &= g\mu - (\delta + \eta_2 I)S_2, \\ F_3(T) &= (\eta_1 S_1 + \eta_2 S_2)I - (\beta + \delta)E, \\ F_4(T) &= \beta E - (\gamma + \delta + \theta)I, \\ F_5(T) &= \gamma I - \delta R. \end{aligned} \tag{6}$$

Based on triangle inequality, one has

$$\begin{aligned} &\| F(T) - F(\bar{T})\| \leq L_1|(\bar{S_1} - S_1)| + L_2|(\bar{S_2} - S_2)| + L_3|(\bar{E} - E)| + L_4|(\bar{I} - I)| + \\ &\quad L_5|(\bar{Q} - Q)| + \delta|(\bar{R} - R)| \leq L\|T - \bar{T}\|, \end{aligned} \tag{7}$$

where

$L_1 = 2\eta_1 + \delta, L_2 = 2\eta_2 + \delta, L_3 = 2\beta + \delta, L_4 = 2\eta_1 + 2\eta_2 + 2\gamma + \delta + \theta$, and $L = max\{L_1, L_2, L_3, L_4, \delta\}$.

3.2 Parameter Estimation

In this subsection, we estimate several parameters in Eq. (1) using the least squares method [25], [26], [27]. The estimation is based on diphtheria case data in Indonesia from 2012 to 2023 [8]. Fig. 2 presents a comparison between the simulation results from Eq. (1) and the actual reported diphtheria cases over the same period. Eq. (1) involves eight parameters, including three demographic parameters μ (birth rate), g(proportion of vaccinated individuals), and δ (natural death rate), which we estimate based on demographic data in Indonesia from 2012 to 2023. The remaining five parameters, namely $\eta_1, \eta_2, \beta, \gamma$, and θ, are obtained through a model fitting process, based on diphtheria case data, as summarized in Table 2 [28].

In 2023, the estimated number of individuals in Indonesia aged 0 to 9 years (N) was 44,511,900 people with an average life expectancy of 72.18 years. The total number of births (u) of 4,030,995 people, and the number of vaccinated individuals within 0 to 9 age (p) of 26,337,314 people. Using these data, we calculated the parameter values μ, g and δ, resulting in $\mu = \frac{u}{N} = 0.1$, $g = \frac{p}{N} \approx 0.6$ and $\delta = \frac{1}{72.18}$ per year.

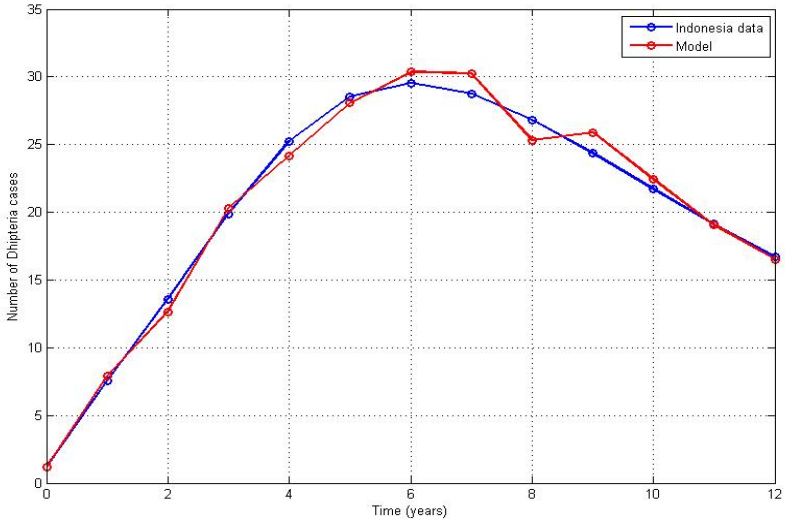

Figure 2. Fitting Model of Diphtheria Cases in Indonesia

Based on the estimation results shown in Table 2, the Mean Absolute Percentage Error (MAPE) between the data and the model solution for diphtheria cases in Indonesia is 8.77%. The initial conditions of the population in the simulation are assumed to be as follows ($S_1(0) = 12.7$, $S_2(0) = 30$, $E(0) = 15.5$, $I(0) = 1.19$, dan $R(0) = 0$). The other five parameters are estimated using the Least Squares method on cumulative data. The parameters (μ, g, δ) were estimated because the data was available at [28]-[30] and could be measured. These parameters, particularly the natural birth and death rates (not due to diphtheria), could not be controlled through disease control efforts. Meanwhile, the parameters $(\eta_1, \eta_2, \beta, \gamma, \theta)$ are obtained through a fitting process against diphtheria case data, as these parameters are dynamic and influenced by control measures such as isolation, contact restrictions, and vaccination coverage. All estimated parameter values are shown in Table 2.

Tabel 2. Fitted and Estimated Values of the Parameters

Parameters	Value	Source
μ	0.1	Estimated [28], [29], [30]
g	0.6	Estimated [28], [29], [30]
δ	0.01	Estimated [28], [29], [30]
η_1	0.0368	Fitted
η_2	0.0317	Fitted
β	0.4530	Fitted
γ	0.1281	Fitted
θ	0.1281	Fitted

3.3 Equilibrium Point

An equilibrium point represents a condition in which the population of each compartment remains constant over time, meaning their rates of change are zero. Based on this definition, the diphtheria transmission model satisfies the condition for a disease-free equilibrium (DFE), denoted by ε_0. This equilibrium occurs when the disease is absent from the population, implying that the number of infected individuals is zero, or $I = 0$. The system of Eq. (1) has the following disease-free equilibrium point ε_0 given as

$$\varepsilon_0 = (S_1^0, S_2^0, E^0, I^0, R^0) = \left(\frac{(1-g)\mu}{\delta}, \frac{g\mu}{\delta}, 0,0,0\right). \quad (8)$$

The basic reproduction number $\mathcal{R}_0$ represents the average number of secondary infections caused by a single infected individual in a fully susceptible population. If $\mathcal{R}_0 < 1$, each infected person transmits the disease to fewer than one individual on average, preventing the spread of the infection and leading to its eventual elimination from the population. Conversely, if $\mathcal{R}_0 > 1$, each infected person infects more than one individual on average, allowing the disease to persist and become endemic. The value of $\mathcal{R}_0$ is calculated by

determining the dominant eigenvalue of the Next Generation Matrix [31]. Through linearization around the disease-free equilibrium point ε_0, we obtain:

$$J = \begin{pmatrix} 0 & (\eta_1 S_1 + \eta_2 S_2) \\ 0 & 0 \end{pmatrix} - \begin{pmatrix} (w\beta + \delta) & 0 \\ -\beta & (\gamma + \theta + \delta) \end{pmatrix}, \\ = F - V. \tag{9}$$

Here, F denotes the transmission matrix representing new infections, while V represents the transition matrix describing the movement of individuals between compartments. Consequently, the basic reproduction number $\mathcal{R}_0$ is defined as the spectral radius of the matrix product FV^{-1}, i.e., its dominant eigenvalue. Thus, the basic reproduction number for system of Eq. (1) is given by:

$$\mathcal{R}_0 = \frac{(\eta_1(1-g) + \eta_2 g)\beta\mu}{\delta(\beta + \delta)(\gamma + \theta + \delta)}. \tag{10}$$

3.4 Stability of Disease-Free Equilibrium Point

This subsection presents the local stability analysis of the equilibrium point under disease-free conditions. In such conditions, the equilibrium is considered stable if all eigenvalues of the system are negative [32]. The Jacobian matrix of Eq. (1), evaluated at the disease-free equilibrium point ε_0 is expressed as

$$J(\varepsilon_0) = \begin{pmatrix} -\delta & 0 & 0 & -\frac{\eta_1(1-g)\mu}{\delta} & 0 \\ 0 & -\delta & 0 & -\frac{\eta_2 g\mu}{\delta} & 0 \\ 0 & 0 & -a_1 & \frac{(\eta_1(1-g)+\eta_2 g)\mu}{\delta} & 0 \\ 0 & 0 & \beta & -a_2 & 0 \\ & & & \gamma & -\delta \end{pmatrix}, \tag{11}$$

where $a_1 = \beta + \delta$ and $a_2 = \gamma + \delta + \theta$. The characteristic equation can be determined by $|J(\varepsilon_0) - \lambda I| = 0$, then we obtain

$$(\lambda + \delta)^3\left(\lambda^2 + (a_1 + a_2)\lambda + a_1 a_2(1 - \mathcal{R}_0)\right) = 0. \tag{12}$$

Eigenvalues of Eq. (12) are $\lambda_1 = \lambda_2 = \lambda_3 = -\delta$, the two eigenvalues are determined by the roots of the following equation:

$$\lambda^2 + m_1\lambda + m_2 = 0, \tag{13}$$

where $m_1 = a_1 + a_2$ and $m_2 = a_1 a_2(1 - \mathcal{R}_0)$.

By using *Routh-Hurwitz* criteria [33], the Eq. (13) has negative real roots, if and only if $m_1, m_2 > 0$. Clear that $m_1 > 0$ and $m_2 > 0$ because a_1 and a_2 are positive for $\mathcal{R}_0 < 1$. So, the Eq. (13) has two negative real roots. As a result, the disease-free equilibrium points ε_0 in Eq. (1) is locally asymptotically stable for $\mathcal{R}_0 < 1$ and unstable for $\mathcal{R}_0 \geq 1$.

3.5 Global Stability of Disease-Free Equilibrium Point

In analyzing the dynamics of epidemic models, establishing the global stability of S_1S_2EIR is essential for understanding disease transmission and evaluating the impact of control strategies. One theoretical method used to ensure global stability involves constructing Lyapunov functions, which provide a means to demonstrate the global convergence of solutions toward either the disease-free or endemic equilibrium. The proposed Lyapunov function candidates are defined as follows [34], [35]:

$$V(t) = \left(S_1 - S_1^0 - S_1^0 \ln\left(\frac{S_1}{S_1^0}\right)\right) + \left(S_2 - S_2^0 - S_2^0 \ln\left(\frac{S_2}{S_2^0}\right)\right) + \frac{\beta E}{\beta+\delta} + E + I + \left(R - R^0 - R^0 \ln\left(\frac{R}{R^0}\right)\right). \quad (14)$$

Based on LaSalle's invariance principle in [36] and $I = \frac{\beta E}{(\gamma+\delta+\theta)}, R^* = \frac{\gamma I}{\delta}, \mathcal{R}_0 = \frac{\beta\mu\left(\eta_1(1-g)+\eta_2 g\right)}{\delta(\beta+\delta)(\gamma+\theta+\delta)}$, which implies that

$$D_*^\alpha V(t) \leq -\delta\left(\frac{\left(S_1 - S_1^0\right)^2}{S_1}\right) - \delta\left(\frac{\left(S_2 - S_2^0\right)^2}{S_2}\right) + (\gamma+\delta+\theta)(R_0 - 1)I + (\beta+\delta)(R_0 - 1)E. \quad (15)$$

Clear that $D_*^\alpha V(t) < 0$ if $\mathcal{R}_0 < 1$. So, the disease-free equilibrium point in Eq. (1) is globally asymptotically stable. The discussion above can be summarized in the following theorem:

Theorem 2. *If $\mathcal{R}_0 < 1$, the disease-free equilibrium point ε_0 in Eq. (1) is globally asymptotically stable.*

3.6 Endemic Equilibrium

In this sub-chapter, the endemic equilibrium point ε_1 of Eq. (1) occurs when the infected sub-population I^* does not have a value of zero. By substituting I^* into Eq. (1), one can get

$$\varepsilon_1 = \left(S_1^*, S_2^*, E^*, I^*, R^*\right) = \left(\frac{(1-g)\mu}{\left(\delta+\eta_1 I^*\right)}, \frac{g\mu}{\left(\delta+\eta_2 I^*\right)}, \frac{\mu I^*\left(\frac{\eta_1(1-g)}{\left(\delta+\eta_1 I^*\right)} + \frac{\eta_2 g}{\left(\delta+\eta_2 I^*\right)}\right)}{(\beta+\delta)}, I^*, \frac{\gamma I^*}{\delta}\right), \quad (16)$$

with I^* is the solution to the following equation:

$$AI^{*2} + BI^* + C = 0, \quad (17)$$

where $A = \eta_1\eta_2$, $\mathrm{B} = \delta\left(\left(\eta_1+\eta_2\right) - \frac{\mathcal{R}_0}{\eta_1(1-g)+\eta_2 g}\right)\eta_1\eta_2$, and $\mathrm{C} = \delta^2\left(1-\mathcal{R}_0\right)$. Clear that, $A > 0$ and $C < 0$ for $R_0 > 1$. Based on Vieta's theorem, the solution of Eq. (17) can be obtained. We divide three cases for the value of B:

1. Case $B = 0$, the solution to Eq. (17) can be obtained as follows:

$$I^* = \sqrt{\frac{\delta^2(\mathcal{R}_0 - 1)}{\eta_1\eta_2}}. \quad (18)$$

If $R_0 > 1$, then the value of I^* will be a real positive, it's meaning the spread of the disease is still occurs in the population.

2. Case $B > 0$, the solution to Eq. (17) is

$$I^* = \frac{-B + \sqrt{D}}{2\eta_1\eta_2}. \quad (19)$$

where

$$B = \delta\left(\left(\eta_1+\eta_2\right) - \frac{\mathcal{R}_0}{\eta_1(1-g)+\eta_2 g}\right)\eta_1\eta_2 \text{ dan } D = B^2 + 4\eta_1\eta_2\delta^2(\mathcal{R}_0 - 1).$$

3. Case $B < 0$, the solution to Eq. (17) is

$$I^* = \frac{B+\sqrt{D}}{2\eta_1\eta_2}, \quad (20)$$

where

$$B = \delta\left(\left(\eta_1 + \eta_2\right) - \frac{\mathcal{R}_0}{\eta_1(1-g)+\eta_2 g}\right)\eta_1\eta_2 \text{ dan } D = B^2 + 4\eta_1\eta_2\delta^2\left(\mathcal{R}_0 - 1\right).$$

If $R_0 = 1$, as a result $\mathrm{C} = 0$, the solution to Eq. (17) is $I^* = -\delta\left(\eta_1 + \eta_2\right) + \frac{\beta\mu}{\mathcal{R}_0(\beta+\delta)(\gamma+\theta+\delta)}$. The value of I^* will be a real negative if $\delta\left(\eta_1 + \eta_2\right) > \frac{\beta\mu}{\mathcal{R}_0(\beta+\delta)(\gamma+\theta+\delta)}$.

3.7 Endemic Global Stability

The global stability of endemic Eq. (1) is also discussed in this study. The Lyapunov function is defined $V: \Omega\backslash\Omega_0 \to \mathbb{R}$ as follows [34], [35]:

$$V(t) = \sigma_1(S_1(t)) + \sigma_2(S_2(t)) + \sigma_3(E(t)) + \sigma_4(I(t)) + \sigma_5(R(t)) \tag{21}$$

where

$$\sigma_1\left(S_1(t)\right) = S_1 - S_1^* - S_1^* \ln\left(\frac{S_1}{S_1^*}\right), \sigma_2\left(S_2(t)\right) = S_2 - S_2^* - S_2^* \ln\left(\frac{S_2}{S_2^*}\right),$$

$$\sigma_3\left(E(t)\right) = E - E^* - E^* \ln\left(\frac{E}{E^*}\right), \sigma_4\left(I(t)\right) = I - I^* - I^* \ln\left(\frac{I}{I^*}\right), \text{ and } \sigma_5(R(t)) = R - R^* - R^* \ln\left(\frac{R}{R^*}\right).$$

The endemic equilibrium point of the Eq. (1) is globally asymptotically stable if $D_*^\alpha V(t) < 0$. By LaSalle's invariance principle in [36], one can derive:

$$D_*^\alpha V(t) \le \rho_1 + \rho_2 + \rho_3 + \rho_4 + \rho_5 \tag{22}$$

where

$$\rho_1 = \left(1 - \frac{S_1^*}{S_1}\right)\left((1-g)\mu - (\delta + \eta_1 I)S_1\right), \rho_2 = \left(1 - \frac{S_2^*}{S_2}\right)(g\mu - (\delta + \eta_2 I)S_2),$$

$$\rho_3 = \left(1 - \frac{E^*}{E}\right)\left((\eta_1 S_1 + \eta_2 S_2)I - (\beta + \delta)E\right), \rho_4 = \left(1 - \frac{I^*}{I}\right)(\beta E - (\gamma + \delta + \theta)I), \text{ and}$$

$$\rho_5 = \left(1 - \frac{R^*}{R}\right)(\gamma I - \delta R).$$

By assuming $S_1 = S_1 - S_1^*, S_2 = S_2 - S_2^*, E = E - E^*, I = I - I^*$, and $R = R - R^*$, we obtain

$$\begin{aligned} D_*^\alpha V(t) \le\ & \mu + \mu\frac{S_1^*}{S_1} + g\mu\frac{S_1^*}{S_1} + g\mu\frac{S_2^*}{S_2} + \delta\left(\frac{(S_1 - S_1^*)^2}{S_1}\right) + \delta\left(\frac{(S_2 - S_2^*)^2}{S_2}\right) + \eta_1 I\left(\frac{(S_1 - S_1^*)^2}{S_1}\right) \\ & + \eta_1 I^*\left(\frac{(S_1 - S_1^*)^2}{S_1}\right) + \eta_2 I\left(\frac{(S_2 - S_2^*)^2}{S_2}\right) + \eta_2 I^*\left(\frac{(S_2 - S_2^*)^2}{S_2}\right) + \eta_1 S_1 I + \eta_1 S_1^* I \\ & + \eta_1 S_1 I^* + \eta_1 S_1^* I^* + \eta_1\frac{E^*}{E}S_1 I + \eta_1\frac{E^*}{E}S_1^* I + \eta_1\frac{E^*}{E}S_1 I^* + \eta_1\frac{E^*}{E}S_1^* I^* + \eta_2 S_2 I + \eta_2 S_2^* I \\ & + \eta_2 S_2 I^* + \eta_2 S_2^* I^* + \eta_2\frac{E^*}{E}S_2 I + \eta_2\frac{E^*}{E}S_2^* I + \eta_2\frac{E^*}{E}S_2 I^* + \eta_2\frac{E^*}{E}S_2^* I^* \\ & + a_1\left(\frac{(E - E^*)^2}{E}\right) + \beta E + \beta E^* + \beta E\frac{I^*}{I} + \beta E^*\frac{I^*}{I} + a_2\left(\frac{(I - I^*)^2}{I}\right) + \gamma I + \gamma I^* + \gamma I\frac{R^*}{R} \\ & + \gamma I^*\frac{R^*}{R} + \delta\left(\frac{(R - R^*)^2}{R}\right). \end{aligned}$$

Making simplification of this calculation, one has

$$D_*^\alpha V(t) \le \mathcal{H}_1 - \mathcal{H}_2, \tag{23}$$

where

$$\mathcal{H}_1 = \mu + \eta_1\left(S_1 I + S_1^* I^* + \frac{E^*}{E} S_1^* I + \frac{E^*}{E} S_1 I^* + \frac{(S_1 - S_1^*)^2}{S_1} I^*\right) + \eta_2\left(S_2 I + S_2^* I^* + \frac{E^*}{E} S_2^* I + \frac{E^*}{E} S_2 I^* + \frac{(S_2 - S_2^*)^2}{S_2} I^*\right) + \gamma\left(I + I^* \frac{R^*}{R}\right) + \beta\left(E + E^* \frac{I^*}{I}\right),$$

and

$$\mathcal{H}_2 = \mu\left(\frac{S_1^*}{S_1} + g\frac{S_1^*}{S_1} - g\frac{S_2^*}{S_2}\right) + \eta_1\left(S_1 I^* + S_1^* I + \frac{E^*}{E} S_1 I + \frac{E^*}{E} S_1^* I^* + I\frac{(S_1 - S_1^*)^2}{S_1}\right) + \eta_2\left(S_2^* I + S_2 I^* + \frac{E^*}{E} S_2 I + \frac{E^*}{E} S_2^* I^* + I\frac{(S_2 - S_2^*)^2}{S_2}\right) + \delta\left(\frac{(S_1 - S_1^*)^2}{S_1} + \frac{(S_2 - S_2^*)^2}{S_2} + \frac{(R - R^*)^2}{R}\right) + a_1\left(\frac{(E - E^*)^2}{E}\right) + a_2\left(\frac{(I - I^*)^2}{I}\right) + \gamma\left(I\frac{R^*}{R} + I^*\right) + \beta\left(E\frac{I^*}{I} + E^*\right),$$

we obtain $D_*^\alpha V < 0$ when $\mathcal{H}_1 - \mathcal{H}_2 < 0$.

Moreover, if $S_1 = S_1^*, S_2 = S_2^*, E = E^*, I = I^*$, and $R = R^*$, then $\mathcal{H}_1 - \mathcal{H}_2 = 0$, which implies that $D_*^\alpha V(t) = 0$. Since the condition $I = I^*$ at the endemic equilibrium point can only be achieved when $\mathcal{R}_0 > 1$, the existence of a positive I^* value inherently implies that the fundamental condition $\mathcal{R}_0 > 1$ is satisfied. Consequently, the global stability analysis through this Lyapunov function operates within the domain where $\mathcal{R}_0 > 1$. The invariant set $\{(S_1^*, S_2^*, E^*, I^*, R^*) \in \mathbb{R}_+^5 : D_*^\alpha V(t) = 0\}$ at ε_1 is endemic equilibrium point and based on LaSalle's invariance principle, ε_1 is globally asymptotically stable in $\Omega \backslash \Omega_0$ if $\mathcal{H}_1 - \mathcal{H}_2 < 0$.

3.8 Numerical Simulation

This subsection presents a sensitivity analysis aimed at evaluating the effects of parameter uncertainty and the responsiveness of numerical outcomes to variations in each model parameter. The analysis assumes that all model parameters follow a uniform distribution. Fig. 3 illustrates the parameters influencing the basic reproduction number $\mathcal{R}_0$ in Eq. (1). The figure displays a vertical bar chart representing the sensitivity of each parameter with respect to $\mathcal{R}_0$. Through this analysis, we identify which parameters most significantly affect $\mathcal{R}_0$, thereby enabling the formulation of more focused and effective control strategies. In Fig. 3, the horizontal axis represents the various model parameters, such as β and γ, while the vertical axis shows the relative change in $\mathcal{R}_0$ resulting from 1% increase in each parameter value. Blue bars on the graph indicate both the direction and magnitude of each parameter's effect. Bars above the horizontal axis imply a positive influence on $\mathcal{R}_0$, meaning an increase in the parameter leads to a rise in $\mathcal{R}_0$. Conversely, bars below the axis indicate a negative influence, suggesting that increasing the parameter reduces the value of R₀. Table 2 presents the sensitivity index for each parameter with respect to $\mathcal{R}_0$. Based on the parameter values $\mu = 0.1, g = 0.6, \delta = 0.01$, η_1=0.0368, η_2=0.0317, $\beta = 0.453$, $\gamma = 0.1281$, and $\theta = 0.1281$, the value of $\mathcal{R}_0 = 1.2401$ is obtained.

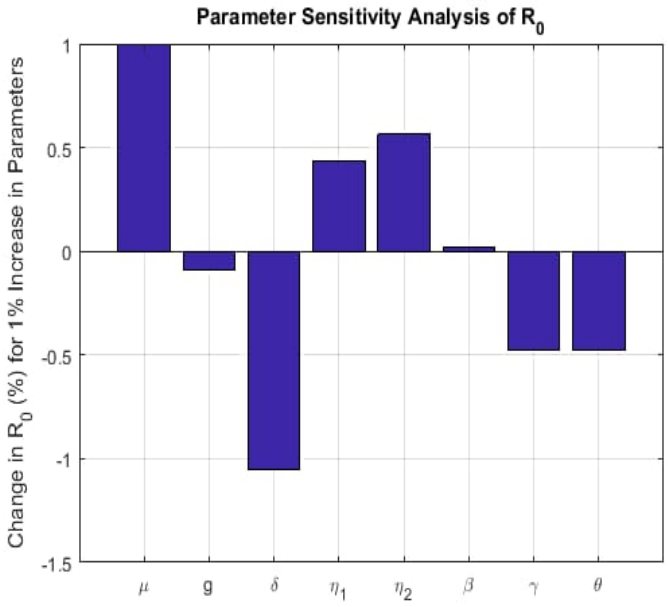

Figure 3. Sensitivity Analysis for $\mathcal{R}_0$ as the Response Function

Table 3. Sensitivity Index of Parameters

Parameters	Sensitivity index
$\boldsymbol{\mu}$	1
$\boldsymbol{g}$	-0.09
$\boldsymbol{\delta}$	-1.05
$\boldsymbol{\eta_1}$	0.44
$\boldsymbol{\eta_2}$	0.56
$\boldsymbol{\beta}$	0.02
$\boldsymbol{\gamma}$	-0.48
$\boldsymbol{\theta}$	-0.48

Fig. 4 shows that the parameter μ has a large and positive influence on $\mathcal{R}_0$, meaning that an increase in the value of μ will also increase the value of $\mathcal{R}_0$ significantly. Parameters η_1 and η_2 also have a positive influence, although on a smaller scale. Conversely, parameters δ, γ, θ show a negative influence, meaning that these values will decrease $\mathcal{R}_0$. Among the three parameters, δ has the largest negative influence, making it a parameter that can control transmission. Other parameters such as β and g show a very small influence on $\mathcal{R}_0$, both positive and negative, so they are not very significant in influencing the dynamics of disease spread in this model.

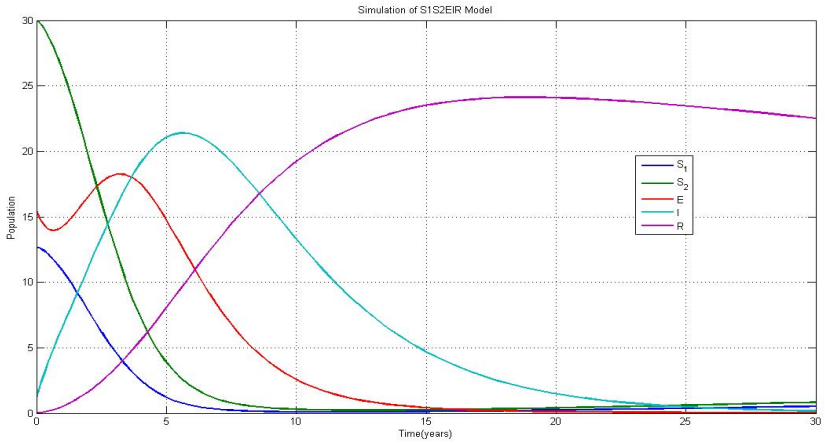

Figure 4. S_1S_2EIR Model and Their Effects on Population Growth Over Time

Furthermore, this study also conducted a numerical simulation of Eq. (1) using the initial conditions used for the model adjustment process and the model parameter values obtained from the adjustment process as presented in Table 2. Fig. 4 shows the results of the numerical simulation of the SEIR model modified into the S_1S_2EIR model. This graph illustrates the population changes in each compartment from time $t = 0$ to $t = 30$. At the beginning of the simulation (t approaching 0), the population I increased sharply from a value close to zero to a peak of almost 25 at around $t = 7$. This increase reflects the very rapid spread of infection at the beginning of the epidemic. However, after the peak was reached, the population I decreases but does not converge to zero starting from time $t = 10$. Instead, it approaches a small positive value, consistent with the analytical result that, for $\mathcal{R}_0 = 1.24 > 1$, the endemic equilibrium is globally asymptotically stable. This means that the number of active infections implying the disease will remain in the population case.

The population R also experiences a rapid increase as I increases, as individuals recovering from infection move to compartment R. The maximum value of R is reached around $t = 18$ with a number of around 23, then slowly decreases and finally stabilizes near 20 at $t > 30$. This decrease indicates that no more individuals move from I to R because the infection has stopped spreading. Meanwhile, the populations S_1 and S_2, which represent susceptible individuals without and with vaccination respectively, show an increasing trend after I approaches 0. The population S_1 and S_2 stabilizes at around $t > 30$. This indicates that part of the population remains susceptible but is not infected because disease transmission has been stopped. The population E, which is individuals who have been exposed but have not transmitted the disease, shows a pattern similar to I. The population E increases initially, then decreases and finally approaches zero around $t = 15$, indicating that there is no more active transmission.

The parameter variations are carried out over a period of 11 years (2012 to 2023) when diphtheria was reported in Indonesia. This helps predict the dynamics of the disease in the country in the next years that are not recorded by the data. Simulations of parameter variations $\eta_1, \eta_2, \mu, \gamma$ and θ are shown in Fig. 5. Fig. 5 (a) illustrates the impact of parameter η_1 (interaction rate between unvaccinated and infected individuals) on infection dynamics (I). From the graph it can be seen that the greater the value of η_1, the higher the peak number of infected population and is achieved in a faster time, demonstrating the critical role of unvaccinated population interactions with infected individuals in accelerating disease transmission. The curve with $\eta_1 = 0.05$ shows the highest peak compared to $\eta_1 = 0.03$ and $\eta_1 = 0.01$, which shows that the higher the interaction of vulnerable groups, the greater the potential for an outbreak. However, at a certain time $t = 11$, $\eta_1 = 0.01$ shows an increase compared to others. This can occur due to an adaptation mechanism, where a large portion of the population becomes immune to a disease after many people have been vaccinated or infected.

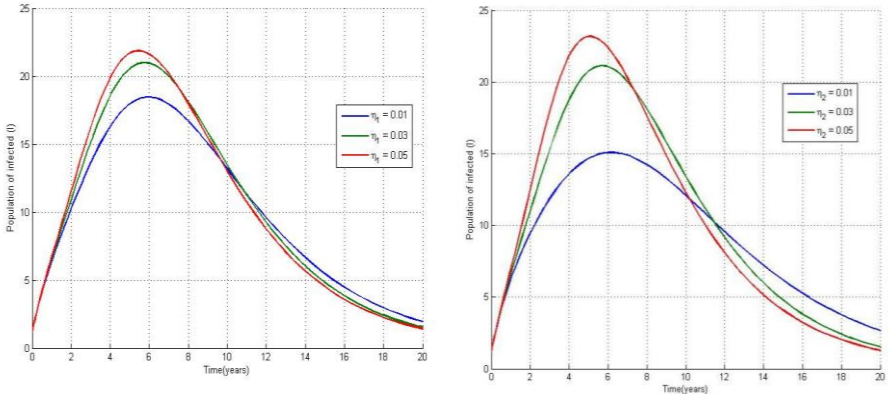

(a) (b)

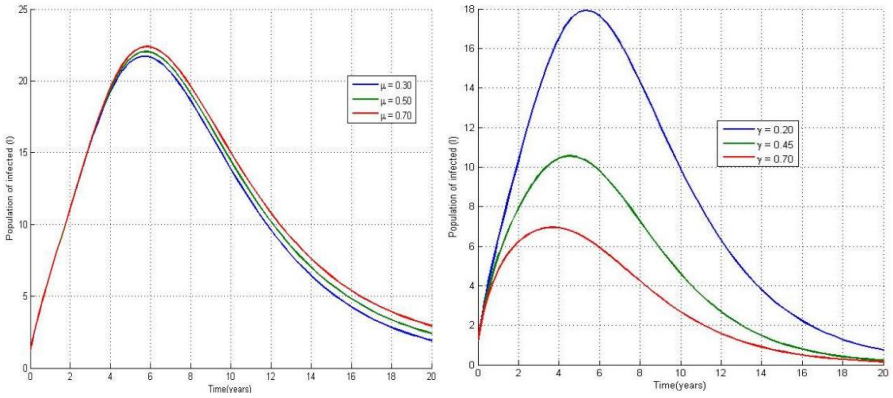

(c) (d)

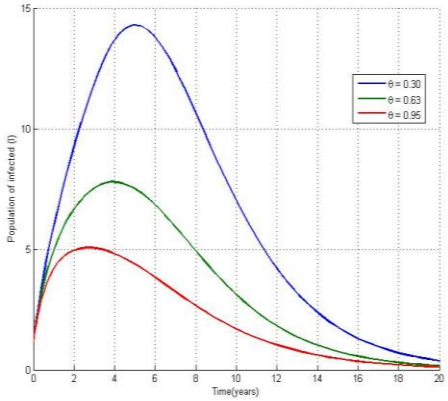

(e)

Figure 5. The Effect of Parameter to Population I

(a) The Effect of Parameter η_1 to Population I, (b) The Effect of Parameter η_2 to I, (c) The Effect of Parameter μ to Population I, (d) The Effect of Parameter γ to Population I, (e) The Effect of Parameter θ to Population I

Fig. 5 (b) shows the effect of variation in η_2, which is the rate of interaction between vaccinated individuals and infected individuals. In general, the graph shows that an increase in the value of η_2 also causes an increase in the number of infected populations, although not as large as the impact of η_1. This indicates that although vaccinated individuals are still potentially infected, protection from vaccination is still able to reduce the rate of spread. Compared to η_1, variation in η_2 results in a slower increase in infections and with a lower peak, emphasizing the importance of vaccination coverage in slowing the spread of infection. Fig. 5 (c) demonstrates the effect of the birth rate μ on the number of infected individuals. Higher μ values lead to higher infection peaks due to the increased influx of susceptible individuals, which increases transmission opportunities. Although the time to reach the peak of infection is relatively unchanged, the height of the peak of infection shows that the increase in the susceptible population increases the burden of infection in society.

Fig. 5 (d) shows the effect of variation of parameter γ, namely the recovery rate on the dynamics of the infected population. The graph in Fig. 5 (d) shows that the lower the value of γ, the lower the peak number of infected individuals and the time to reach the peak becomes faster. This makes sense because an increase in the recovery rate means that infected individuals move to the recovered group more quickly, thereby reducing the number of individuals in the active infection group. In other words, increasing γ can accelerate the population recovery process and reduce pressure on the health system. Fig. 5 (e) shows the variation of the parameter θ, which is the death rate due to diphtheria. Higher θ values reduce the infection peak because infected individuals die more quickly, resulting in a shorter infectious period. Although technically this reduces the number of active infections, of course increasing the value of θ is not a medically desirable solution. However, from the perspective of model dynamics, θ remains an important parameter that must be considered in designing strategies for controlling and mitigating the impact of the disease.

Thus, Fig. 5 comprehensively show that changes in the parameters have a significant impact on the pattern of diphtheria spread. The greatest impact on the peak of infection is shown by an increase in the transmission rate (β) and a decrease in the cure rate (γ), while effective interventions can be focused on increasing vaccination (reducing η) and increasing the speed of medical treatment (increasing γ).

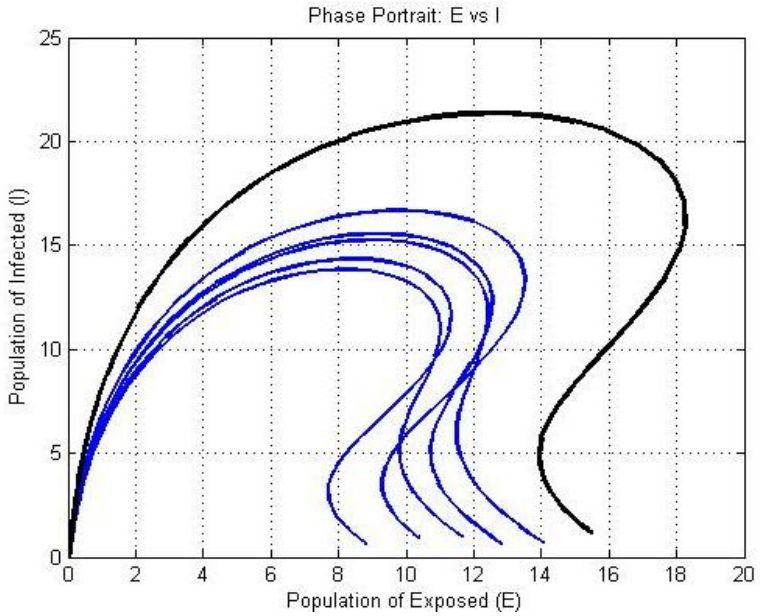

Figure 6. Phase Portrait of the Diphtheria Epidemic Model

Furthermore, this study also analyzes the phase portrait of the diphtheria epidemic model by representing the complex dynamics between the exposed (E) and infected (I) populations through a series of trajectories that describe the evolution of the system over time. The horizontal axis represents the value of E (the number of exposed populations), while the vertical axis represents the value of I (the number of infected populations). The curves of the phase portraits are shown in Fig. 6. Fig. 6 explains the various initial conditions and represents the solution trajectories of the nonlinear differential system over time. Each curve shows the direction of change of the pair (E, I) as the system evolves, and provides an understanding of how the exposed and infected populations change together. Fig. 6 also shows that most trajectories start from low E values and low I values. These trajectories then move up, indicating that an increase in the number of exposed individuals (E) causes a spike in the number of infected individuals (I). This is in accordance with the natural dynamics of disease spread, namely the more exposed, the greater the likelihood of increasing infection. However, after a certain point, when the E value begins to decrease, the I value remains high for a moment before finally decreasing. This suggests a delay between the peak number of exposed individuals and the peak of active infections (a common phenomenon in infectious diseases that have an incubation period).

Some trajectories display a rounded or semi-spiral pattern, indicating a tendency for the system to move towards equilibrium. This means that in the long run, the system will reach a stable state where the number of individuals in E and I no longer changes significantly. This phenomenon indicates that the disease can persist as an endemic disease, depending on the values of parameters such as infection rate, recovery, and mortality. The thinner trajectories show variations in dynamics due to differences in initial conditions, while the one thick black trajectories represent the main dynamics of the system, based on initial conditions. This trajectories pass through maximum values in both E and I before decreasing and curving closer to a flat line, indicating the transition from the acute epidemic phase to stability.

4. CONCLUSION

This study successfully developed and analyzed a mathematical model of diphtheria transmission that incorporates different susceptibility levels within the Indonesian population. The model demonstrates that high vaccination coverage significantly reduces disease transmission, with the basic reproduction number $\mathcal{R}_0 = 1.2401$ indicating endemic potential under current conditions. Numerical simulations revealed that the

interaction rate among unvaccinated individuals (η_1) serves as a critical outbreak driver, with elevated values correlating with infection peaks 2-3 times higher than baseline scenarios. The analytical framework established that global stability at the disease-free equilibrium point ε_0 is achieved when $\mathcal{R}_0 < 1$. Conversely, the system tends toward the endemic equilibrium ε_1 when $\mathcal{R}_0 > 1$, and based on LaSalle's invariance principle, ε_1 is globally asymptotically stable in $\Omega \backslash \Omega_0$ if $\mathcal{H}_1 - \mathcal{H}_2 < 0$. Parameter estimation through least-squares fitting results presented in Fig. 2 yielded strong alignment between model predictions and empirical data from 2012-2023, validating the model's accuracy in capturing diphtheria dynamics in Indonesia.

From a policy perspective, these findings underscore the importance of targeted vaccination programs in regions with high interaction rates among unvaccinated populations, coupled with social distancing measures during outbreaks and enhanced surveillance in low-coverage areas. However, this study acknowledges certain limitations, including the assumption of a closed population without migration effects, the deterministic nature of the model that does not account for stochastic variations in disease transmission, and the homogeneous mixing assumption that may not fully capture complex social interaction patterns. Future research directions should incorporate spatio-temporal analysis to address geographical spread patterns, develop stochastic frameworks to better capture parameter uncertainty, and Integration of real-world diphtheria case data from Indonesia. These advancements would further strengthen the mathematical foundation for developing precise, efficient, and sustainable diphtheria control measures in Indonesia and similar settings.

Author Contributions

Mohamad Tafrikan: Conceptualization, Writing-Original Draft, Software, Validation. Fatmawati: Methodology, Data Curation, Resources, Draft Preparation. Windarto: Formal Analysis, Validation, Chinwendu E. Mudubueze: Software, Visualization, Writing-Review and Editing. All authors discussed the results and contributed to the final manuscript.

Funding Statement

The first author was supported by Beasiswa Indonesia Bangkit - Education Fund Management Institution (LPDP)-Ministry of Religion of the Republic of Indonesia with number REG20250519017.

Acknowledgment

The author hereby expresses his gratitude to all parties who have contributed to the success of this research, especially to the reviewers who have provided constructive suggestions.

Declarations

The authors declare no competing interest.

Declaration of Generative AI and AI-assisted Technologies

The authors declare that no generative AI or AI-assisted technologies were used in the preparation of this manuscript, including for writing, editing, data analysis, or the creation of tables and figures

REFERENCES

[1] WHO, “DIPHTHERIA.” Accessed: Jun. 10, 2024. [Online]. Available: https://www.who.int/news-room/questions-and-answers/item/diphtheria

[2] Ministry of Health of the Republic of Indonesia, “GUIDELINES FOR PREVENTION AND CONTROL OF DIPHTHERIA.” Accessed: Jun. 11, 2024. [Online]. Available: https://www.cdc.gov/diphtheria/about/?CDC_AAref_Val

[3] Anderson, “WHAT TO KNOW ABOUT DIPHTHERIA.” Accessed: Jun. 10, 2024. [Online]. Available: https://www.webmd.com/a-to-z-guides/what-to-know-diphtheria-causes.

[4] National Health Service, “DIPHTHERIA.” Accessed: Jun. 10, 2024. [Online]. Available: https://www.nhs.uk/conditions/diphtheria/.

[5] Centers for Disease Control and Prevention, “DIPHTHERIA.” [Online]. Available:

https://www.cdc.gov/diphtheria/about/?CDC_AAref_Val=https://www.cdc.gov/diphtheria/about/causes-transmission.html
[6] K. Rogers, "DIPHTHERIA," The Editors of Encyclopaedia Britannica. Accessed: Jul. 10, 2024. [Online]. Available: https://www.britannica.com/science/diphtheria.
[7] S. R. Lamichhane, "DIPHTHERIA," StatPearls. Accessed: Sep. 15, 2025. [Online]. Available: https://www.ncbi.nlm.nih.gov/books/NBK560911/.
[8] Ministry of Health of the Republic of Indonesia, "INDONESIAN HEALTH PROFILE 2023." Accessed: Jun. 12, 2024. [Online]. Available: https://kemkes.go.id/id/category-download/profil-kesehatan
[9] T. Witelski and M. Bowen, "METHODS OF MATHEMATICAL MODELLING: CONTINUOUS SYSTEMS AND DIFFERENTIAL EQUATIONS," *Contin. Syst. Differ. Equations*, pp. 23–45, 2015. doi : https://doi.org/10.1007/978-3-319-23042-9_2
[10] F. Brauer, C. Castillo-Chavez, F. Brauer, and C. Castillo-Chavez, "EPIDEMIC MODELS," *Math. Model. Popul. Biol. Epidemiol.*, pp. 345–409, 2008.doi : https://doi.org/10.1007/978-1-4614-1686-9_9
[11] W. Kermack and A. McKendrick, "A CONTRIBUTION TO THE MATHEMATICAL THEORY OF EPIDEMICS," in *Proceedings of the Royal Society of London 115*, 1927. doi : https://doi.org/10.1098/rspa.1927.0118
[12] H. Hethcote, "THREE BASIC EPIDEMIOLOGICAL MODELS," *Appl. Math. Ecol.*, pp. 119–144, 1989. doi : https://doi.org/10.1007/978-3-642-61317-3_5
[13] G. Puspita, M. Kharis, and Supriyono, "PEMODELAN MATEMATIKA PADA PENYEBARAN PENYAKIT DIFTERI DENGAN PENGARUH KARANTINA DAN VAKSINASI," *Unnes J. Math*, vol. 6, no. 1, p. 26, 2017.
[14] M. Torrea, J. L. Torrea, and D. Ortega, "A MODELING OF A DIPHTHERIA EPIDEMIC IN THE REFUGEES CAMPS", *bioRxiv*, p. 208835, 2017. [Online]. Available: https://www.biorxiv.org/content/10.1101/208835v1, doi : https://doi.org/10.1101/208835
[15] K. Sornbundit, W. Triampo, and C. Modchang, "MATHEMATICAL MODELING OF DIPHTHERIA TRANSMISSION IN THAILAND," *Comput. Biol. Med.*, vol. 87, pp. 162–168, 2017, doi: 10.1016/j.compbiomed.2017.05.031. doi : https://doi.org/10.1016/j.compbiomed.2017.05.031
[16] F. Ilahi and A. Widiana, "THE EFFECTIVENESS OF VACCINE IN THE OUTBREAK OF DIPHTHERIA: MATHEMATICAL MODEL AND SIMULATION," *IOP Conf. Ser. Mater. Sci. Eng.*, vol. 434, no. 1, 2018, doi: 10.1088/1757-899X/434/1/012006. doi : https://doi.org/10.1088/1757-899X/434/1/012006
[17] I. S. Fauzi *et al.*, "ASSESSING THE IMPACT OF BOOSTER VACCINATION ON DIPHTHERIA TRANSMISSION: MATHEMATICAL MODELING AND RISK ZONE MAPPING," *Infect. Dis. Model.*, vol. 9, no. 1, pp. 245–262, 2024, doi: 10.1016/j.idm.2024.01.004. doi : https://doi.org/10.1016/j.idm.2024.01.004
[18] S. O. Adewale, S. O. Ajao, I. A. Olopade, G. A. Adeniran, S. O. Ajao, and I. T. Mohammed, "MATHEMATICAL ANALYSIS OF QUARANTINE ON THE DYNAMICAL TRANSMISSION OF DIPHTHERIA DISEASE SOLVING RICCATI EQUATION USING ADOMIAN DECOMPOSITION METHOD VIEW PROJECT COVID PROJECT VIEW PROJECT IDAYAT TEMILADE MOHAMMED MATHEMATICAL ANALYSIS OF QUARANTINE ON THE," *Int. J. Sci. Eng. Investig.*, vol. 6, no. 64, pp. 8–17, 2017, [Online]. Available: www.IJSEI.com
[19] N. Izzati, A. Andriani, and R. Robi'aqolbi, "OPTIMAL CONTROL OF DIPHTHERIA EPIDEMIC MODEL WITH PREVENTION AND TREATMENT," *J. Phys. Conf. Ser.*, vol. 1663, no. 1, 2020, doi: 10.1088/1742-6596/1663/1/012042.doi : https://doi.org/10.1088/1742-6596/1663/1/012042
[20] N. Rahmi and M. I. Pratama, "MODEL ANALYSIS OF DIPHTHERIA DISEASE TRANSMISSION WITH VACCINATION, QUARANTINE, AND HAND-WASHING BEHAVIOR," *JTAM (Jurnal Teor. dan Apl. Mat.*, vol. 7, no. 2, p. 462, 2023, doi: 10.31764/jtam.v7i2.13466.doi : https://doi.org/10.31764/jtam.v7i2.13466
[21] K. P. Putra and M. Rosha, "MODEL MATEMATIKA TIPE SIQR PENYEBARAN PENYAKIT DIFTERI DENGAN PENGARUH VAKSINASI," *J. Math. UNP*, vol. 7, no. 4, pp. 84–93, 2022. doi : https://doi.org/10.24036/unpjomath.v7i4.13993
[22] M. Sato, R. Ratianingsih, and Hajar, "MEMBANGUN MODEL MATEMATIKA PENYEBARAN PENYAKIT DIFTERI," *J. Ilm. Mat. dan Ter.*, vol. 18, no. 2, pp. 221–229, 2021.doi : https://doi.org/10.22487/2540766X.2021.v18.i2.15705
[23] M. Sholeh, "STABILITY ANALYSIS OF THE SIQR MODEL OF DIPHTHERIA DISEASE SPREAD AND MIGRATION IMPACT," *BAREKENGJournal Math. Its Appl.*, vol. 19, no. 1, pp. 0173–0184, 2025. doi : https://doi.org/10.30598/barekengvol19iss1pp173-184
[24] J. Xu and C. Xue, "UNIQUENESS AND EXISTENCE OF POSITIVE PERIODIC SOLUTIONS OF FUNCTIONAL DIFFERENTIAL EQUATIONS," *AIMS Math.*, vol. 8, no. 1, pp. 676–690, 2023. doi : https://doi.org/10.3934/math.2023032
[25] E. Sinaga, "PENERAPAN METODE LEAST SQUARES METHOD DALAM ESTIMASI PENJUALAN PRODUK ELEKTRONIK," *J. Comput. Informatics Res.*, vol. 2, no. 2, pp. 44–48, 2023. doi : https://doi.org/10.47065/comforch.v2i2.380
[26] H. Motulsky and A. Christopoulos, *Using Global Fitting to Test Treatment Effects*. Oxford: Oxford University Press, 2023.
[27] R. Prasetyo, "IMPLEMENTATION OF THE LEAST SQUARE METHOD FOR POPULATION GROWTH RATE PREDICTION IN AIR SUGIHAN DISTRICT," *J. Inf. Syst. Informatics*, vol. 4, no. 2, pp. 282–299, 2022.doi : https://doi.org/10.51519/journalisi.v4i2.252
[28] Central Statistics Agency of the Republic of Indonesia, "POPULATION BY AGE GROUP AND GENDER." Accessed: Apr. 29, 2025. [Online]. Available: https://www.bps.go.id/id/statistictable/3/WVc0MGEyMXBkVFUxY25KeE9HdDZkbTQzWkVkb1p6MDkjMw==/jumlah-penduduk-menurut-kelompok-umur-dan-jenis-kelamin--ribu-jiwa---2018.html?year=2023
[29] K. W. D. Nugraha, Setiaji, F. Sibuea, and B. Hardhana, *Profil Kesehatan Indonesia*. Jakarta: Kementrian Kesehatan Republik Indonesia, 2021.
[30] C. S. A. of the R. of Indonesia, "LIFE EXPECTANCY BY PROVINCE AND GENDER." Accessed: Apr. 29, 2025. [Online]. Available: https://www.bps.go.id/id/statistics-table/2/NTAxIzI=/angka-harapan-hidup-ahh-menurut-provinsi-dan-jenis-kelamin.html
[31] W. Y. Yang, W. Cao, J. Kim, K. W. Park, H. H. Park, J. Joung, Jong-Suk Ro, H. L. Lee, C. Hong, T. Im. *Applied Numerical Methods Using MATLAB*. John Wiley & Sons, 2020.doi : https://doi.org/10.1002/9781119626879
[32] B. Wei, "STABILITY ANALYSIS OF EQUILIBRIUM POINT AND LIMIT CYCLE OF TWO-DIMENSIONAL

NONLINEAR DYNAMICAL SYSTEMS—A TUTORIAL," *Appl. Sci.*, vol. 13, no. 2, 2023. doi : https://doi.org/10.3390/app13021136

[33] R. Mahardika, Widowati, and Y. D. Sumanto, "ROUTH-HURWITZ CRITERION AND BIFURCATION METHOD FOR STABILITY ANALYSIS OF TUBERCULOSIS TRANSMISSION MODEL," in *Journal of Physics: Conference Series*, Journal of Physics: Conference Series, 2019. doi : https://doi.org/10.1088/1742-6596/1217/1/012056

[34] G. J. Olsder and J. W. van der Woude, *MATHEMATICAL SYSTEMS THEORY*, vol. 4. VSSD Netherlands, 2005.

[35] R. Sundari and E. Apriliani, "CONSTRUCTION OF LYAPUNOV FUNCTIONS TO DETERMINE STABILITY," *J. Sains dan Seni ITS*, vol. 6, no. 1, pp. 1–5, 2017. doi : https://doi.org/10.12962/j23373520.v6i1.22862

[36] K. T. Alligood, T. D. Sauer, J. A. Yorke, and D. Chillingworth, "CHAOS: AN INTRODUCTION TO DYNAMICAL SYSTEMS," *SIAM Rev.*, vol. 40, no. 3, p. 732, 1998.